

Article

Electrospinning-Derived PLA/Shellac/PLA Sandwich—Structural Membrane Sensor for Detection of Alcoholic Vapors with a Low Molecular Weight

Shi-Cai Wang¹, Jun-Wei Liang¹, Ying-Bang Yao^{1,2} , Tao Tao^{1,2}, Bo Liang^{1,2} and Sheng-Guo Lu^{1,2,*} 

¹ Guangdong Provincial Research Center on Smart Materials and Energy Conversion Devices, Guangdong Provincial Key Laboratory of the Functional Soft Condensed Matter, School of Materials and Energy, Guangdong University of Technology, Guangzhou 510006, China; S136544353@163.com (S.-C.W.); 11075351307@163.com (J.-W.L.); ybyao@gdut.edu.cn (Y.-B.Y.); taotao@gdut.edu.cn (T.T.); liangbo@gdut.edu.cn (B.L.)

² Dongguan South China Design Innovation Institute, Building D-1, University Innovation City Area, Songshan Lake, Dongguan 523808, China

* Correspondence: sglu@gdut.edu.cn

Received: 22 October 2019; Accepted: 4 December 2019; Published: 11 December 2019



Featured Application: The sandwich-structural membrane sensor could be used for detection of alcoholic vapors with a low molecular weight.

Abstract: The development of gas sensors for detecting alcoholic vapors with a low molecular weight is essential for environmental protection, industrial process control, and the monitoring of the living atmosphere in daily life to avoid health problems in human beings. Here, poly (lactic acid) (PLA)/shellac/PLA sandwich-structural membranes were fabricated via an electrospinning approach and the interaction with alcoholic vapors with a low molecular weight was investigated. It was found that the PLA/shellac/PLA sandwich-structural membrane exhibited fast response to the alcoholic vapors with low molecular weight, especially for methanol vapor. After being treated with alcohol vapor with a low molecular weight, the PLA/shellac/PLA sandwich-structural membrane could change its transmission in a short time (~5 s) and with a concentration of 10 wt% of methanol (ethanol) in water. In the meantime, the PLA/shellac/PLA sandwich-structural membrane can hopefully be potentially used again after evaporating the alcoholic vapor at an elevated temperature.

Keywords: shellac; electrospinning; sandwich structure; sensor; alcoholic vapor detection

1. Introduction

Gas detection has played an important role in industries, medicines and environment, such as industrial process control [1], environmental pollution monitoring [2], medical respiratory analysis [3,4], and alcoholic detection for drivers (there were 900,000 people who drove after drinking alcohol in the 1st half of 2019 in mainland China) and explosive gas leakage detection [5]. Nowadays, the development of gas sensors, aiming to detecting some unstable toxic vapors, is essential due to the environmental pollution and the safety requirements in the industrial process and daily life. It is well known that alcoholic vapor with a low molecular weight is one of the most common vapors. Inhalation of alcoholic vapor with a low molecular weight can cause damage to the human body. The main damage of methanol to the human body is mainly in the respiratory tract and gastric mucosa. Methanol and its

metabolites have a stimulating effect on the respiratory tract and gastrointestinal mucosa. The vapor can strongly stimulate conjunctiva of the eye. Methanol may also cause toxic effects on vascular nerves, resulting in vasospasm, forming blood stasis and bleeding. In severe cases, due to the cerebral blood circulation disorders and direct effects on the fine nerve sputum, tissue organic lesions may occur. Similarly, ethanol vapor is also harmful to the human body. Exposure to ethanol vapor may cause health problems such as a headache, lethargy, eye irritation, liver damage and difficulty in breathing [6]. Moreover, ethanol inhibits the high activity of the cerebral cortex. Exposure to high concentrations of ethanol vapor also inhibits peripheral nerves. Therefore, it is necessary to develop a sensor for detecting alcoholic vapor concentration with a lower molecular weight. Yebo et al. demonstrated an ethanol vapor sensor using a ZnO nanoparticle film as a coating layer on a SOI (silicon-on-insulator) micro-ring resonator with a radius of 5 μm at room temperature. The partial coating on the ring resonator was prepared using a colloidal suspension of ZnO nanoparticles having a diameter of about 3 nm [7]. Hu et al. reported that the TiO₂ nanobelts were prepared using a hydrothermal treatment, and their surfaces were processed by surface engineering, including surface roughening using an acidic etching process, forming an Ag–TiO₂ heterojunction on the surface of the TiO₂ nanobelts by photoreduction. These researchers managed to test the performance of all samples in ethanol vapor atmosphere and to compare that with the conductivity measurements at a series of temperatures [8]. Patel et al. worked out a method of stimulating ITO (indium-tin-oxide) film recrystallization by depositing an ITO film on an ultra-thin Cu stimulator, which was used to improve the sensitivity, selectivity and minimum detection limit of a methanol sensor operated at room temperature [9]. However, most alcoholic vapor sensors with low molecular weights produced by inorganic materials, metallic oxides and their composites are fabricated using complex processes with high costs, and they cannot work at room temperature in particular. Moreover, these materials are not biodegradable after use, leading to unnecessary environmental pollution. Therefore, better measures should be developed to introduce a new sensor for alcoholic vapor with a low molecular weight through a new approach that is facile, of low cost, and biodegradable, and potentially that can be embedded in clothing.

The electrospinning process is simple and easy to use. The apparatus of electrospinning has a simple structure including a high-voltage power source having a positive or negative polarity, a syringe pump having a capillary tube or a tube to transport the solution from the syringe or pipette to the spinneret, and a conductive collector such as aluminum foil [10]. The electrospinning process uses a high-voltage electric field to produce a charged jet from a polymer solution that produces nanofibers when dried by evaporation of the solvent. The highly charged fibers are directed toward a collector that connects to the ground. During electrospinning, spinning of a fiber is mainly achieved by inducing a tensile force generated in the axial direction of the polymer flow in the presence of an electric field [10–12].

Poly (lactic acid) (PLA) is a thermoplastic, high-strength, high-modulus polymer made from renewable resources in the form of particles, and is widely used for industrial packaging or biocompatible/bioabsorbable medical devices [13,14]. It is easy to process using standard plastic equipment to produce molded parts, films or fibers. Shellac is a kind of resin secreted by the female lac bug on trees in Indian and Thai forests. Due to its excellent water resistance, fixing abilities, film-forming as well as biocompatibility properties, shellac has been widely used in medicine, paint, food, military, dyes and other fields [15]. Compared with traditional technologies, electrospinning is an efficient, simple, and low-cost method for preparing various nanofibers. As mentioned above, shellac is soluble in anhydrous ethanol to make an electrospinning solution. After being treated with the ethanol vapor, the transparency of the shellac electrospinning membrane will be greatly improved [15]. Moreover, PLA electrospinning fibers have been used as stents for drug delivery and tissue engineering due to their high specific surface area [16]. Therefore, the PLA electrospinning membrane was used as a fixed layer, and the shellac electrospinning membrane was combined with the PLA membrane, which is more stable than the shellac membrane itself, and is advantageous for preparing the membrane of the alcoholic vapor sensor with a low molecular weight.

The present study aims to produce an alcoholic vapor sensor with a low molecular weight that is easy to process and test accurately using the PLA/shellac/PLA sandwich-structural membrane via an electrospinning method. In this paper, we report that the PLA/shellac/PLA sandwich-structural membrane will become transparent when exposed to alcoholic vapors with a low molecular weight, in order to detect these at room temperature. Thus an effective and biodegradable sensor can be made to detect the alcoholic vapor with a low molecular weight.

2. Materials and Methods

PLA 6252D ($\rho = 1.24 \text{ g/cm}^3$, the glass transition temperature is at about $58 \text{ }^\circ\text{C}$, NatureWorks, Minnetonka, MN, USA), shellac ($\rho = 1.175 \text{ g/cm}^3$, Bosheng, Beijing, China), dichloromethane (DCM), dimethyl formamide (DMF) and anhydrous ethanol (Tianjin Da Mao Chemical Reagent, Tianjin, China) were used as the two fiber materials and three solvents, respectively. All reagents were utilized without further purification. A plastic syringe (Foshan Lepton Precision Measurement and Control Technology, Foshan, Guangdong, China) with a stainless steel needle (0.50 mm) was employed as the electrospinning equipment. Methanol and anhydrous ethanol (Tianjin Da Mao Chemical Reagent, Tianjin, China) were used for the detecting and sensing of alcoholic vapors with a low molecular weight.

An amount of PLA (10% wt%) was dissolved in a mixture of DCM and DMF (9:1 weight ratio) at room temperature, and stirred for 2 h to form a precursor solution. The precursor was then placed in a plastic syringe of 20 mL in volume and a stainless steel needle of 0.50 mm in diameter was used for electrospinning. The high voltage applied between the tip and the collector was set to 18 kV and the distance between them was 15 cm. The flow rate was fixed as 1.0 mL/h. During the electrospinning process, the temperature was set as $25 \pm 2 \text{ }^\circ\text{C}$ and the relative humidity as $65 \pm 5\%$. After a period of time, the PLA electrospinning membrane on the collector (pure aluminum foil) was removed and dried at room temperature for 8 h. Then, an amount of shellac (45% wt%) was dissolved in anhydrous ethanol at room temperature and stirred for 2 h to form a precursor solution. The solution was then placed in the plastic syringe and the stainless steel needle for electrospinning. Then the shellac membrane was collected on the PLA membrane as prepared. The temperature and humidity were the same as those for the preparation of the PLA membrane. Then, the membrane on the collector was removed and dried at room temperature. After that, a layer of PLA electrospinning membrane was electrospun on the dried membrane, and the parameters of electrospinning were the same as those for the preparation of the PLA membrane. Finally, an electrospinning membrane with a PLA/shellac/PLA sandwich-structure was obtained (see Figure 1).



Figure 1. Schematic illustration of a poly (lactic acid) (PLA)/shellac/PLA sandwich-structural membrane.

A 100 mL alcohol such as methanol or absolute ethanol was added to a specific vessel to fill the vessel with mixed vapors containing alcohol. The specific apparatus is shown in Figure 2. The content of alcohol was constant to ensure that the experiment is carried out in an atmosphere of alcoholic vapor with a low molecular weight and constant concentration. The PLA/shellac/PLA sandwich-structural membrane was then placed in the specific apparatus at room temperature, and the resistance of the

photoresistor was measured after a period of time. The thickness was measured to be $60.2 \pm 0.9 \mu\text{m}$ and $80.4 \pm 1.1 \mu\text{m}$ for PLA and shellac, respectively, using a micrometer.

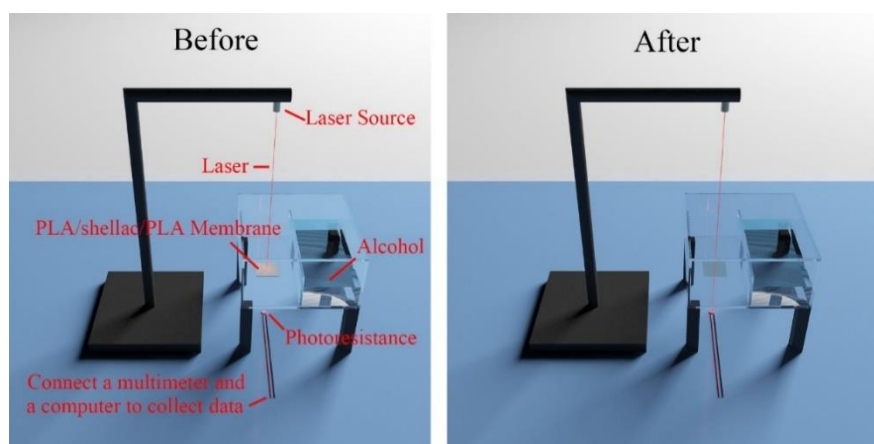


Figure 2. The experimental apparatus and the transparency change of the membrane before and after the treatment with the alcoholic vapor.

In order to accurately measure the resistance value of the photoresistor, the PLA/shellac/PLA sandwich-structural membranes were placed in a single pure vapor at room temperature, and started to test the resistance of the photoresistor.

Scanning electron microscope (SEM) images were taken (SEM, SU8220, Hitachi, Tokyo, Japan). X-ray diffraction (XRD) was carried out on a D/Max-Ultima IV diffractometer (Ultima IV, Rigaku, Tokyo, Japan) over the 2θ range of 10° – 80° . Functional groups of the fibers were measured in absorbance mode by an attenuated total reflection–Fourier transform infrared spectrometer (ATR–FTIR, Nicolet IS50, Thermofisher, Massachusetts, USA). The wavenumber was ranged from 400 to 4000 cm^{-1} . The resistance value of the photoresistor was measured using a multimeter (PM8236, PEAKMETER, Shenzhen, China).

3. Results and Discussion

3.1. Morphology

Figure 3 shows the surface morphology of the pristine electrospun PLA nanofibers before and after alcoholic treatment. The pristine PLA nanofibers were randomly oriented in the SEM image and the average diameters were $2.01 \pm 0.33 \mu\text{m}$. It can be seen that the morphology of the PLA nanofibers does not change significantly after being treated with the alcoholic vapor with a low molecular weight. Figure 4 shows the images of the PLA/shellac/PLA sandwich-structural membrane before and after the treatment with the alcoholic vapor with a low molecular weight. In the experiment, different solution ratios (1 mL/1 mL/1 mL, 1 mL/2 mL/1 mL, 2 mL/1 mL/2 mL) were used. In Figure 4, one can see that, after the treatment, the PLA fiber layers were tightly stuck together, and the shellac nanofiber layer were partially dissolved after the alcoholic vapor treatment. In contrast, the morphology of the PLA nanofibers did not change much after the treatment. For the shellac layer, however, the nanofibers dissolved and slowly penetrated mutually in between the gap until a gap-filling coating was formed on the surface of the PLA membrane. This can explain the reduction in thickness of the composite film after the alcoholic treatment. Figure 5 shows that the PLA/shellac/PLA sandwich-structural membrane changes from opaque to transparent after the treatment of alcoholic vapor with a low molecular weight.

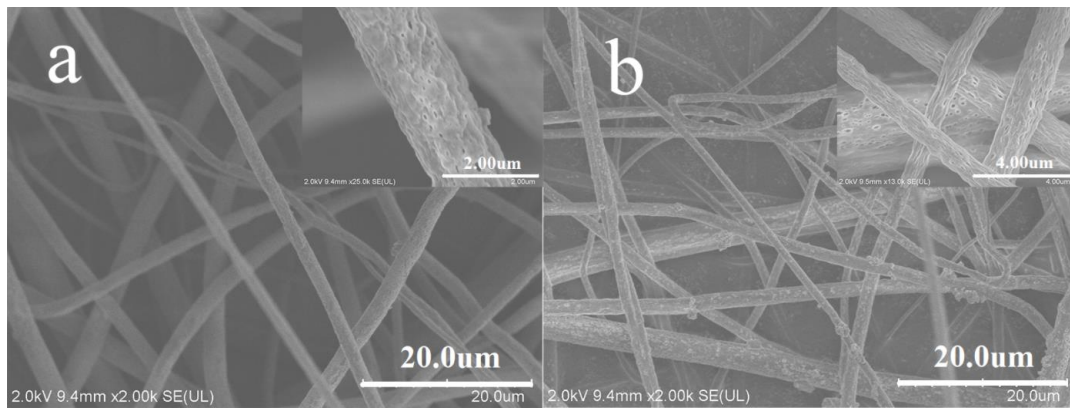


Figure 3. Scanning electron microscope (SEM) images of PLA nanofiber membrane before and after treated with the alcoholic vapor with a low molecular weight. ((a) The left image is $\times 2.00$ k and the inset image is $\times 25.0$ k; (b) the left image is $\times 2.00$ k and the inset image is $\times 13.0$ k).

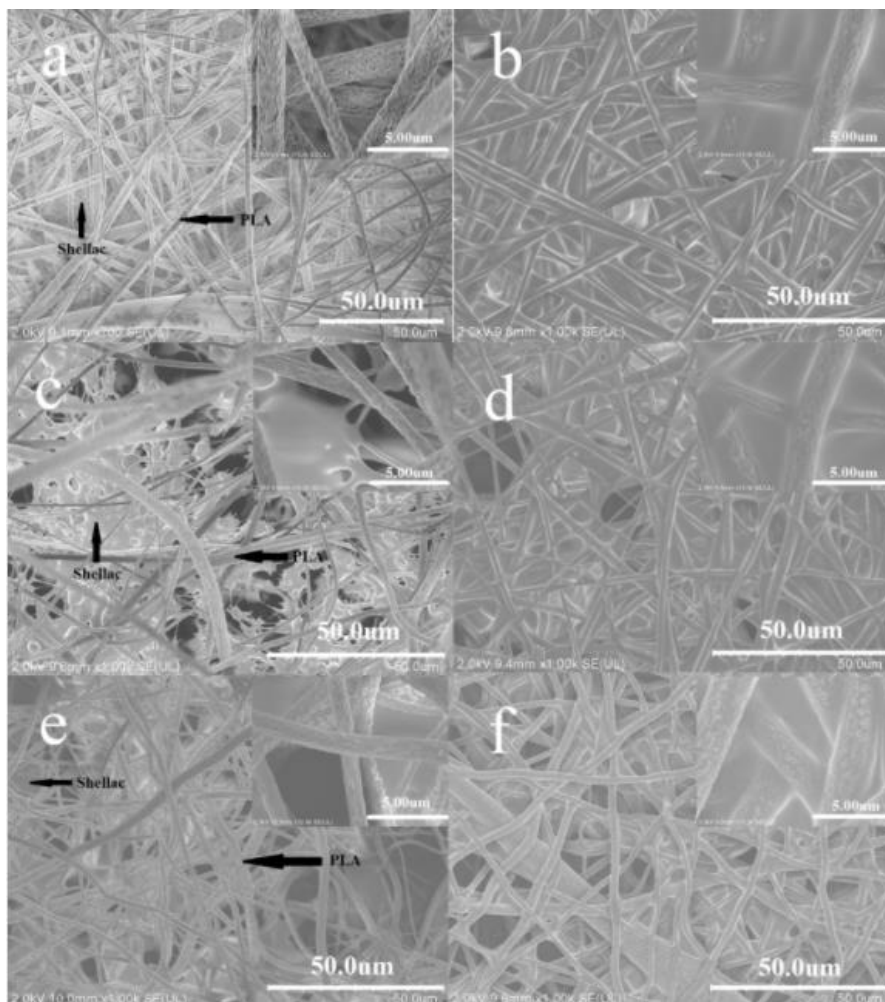


Figure 4. SEM images of the PLA/shellac/PLA sandwich-structural membrane ((a,b) 1 mL/1 mL/1 mL, the left image is $\times 700$ and the inset image is $\times 10.0$ k; (c,d) 1 mL/2 mL/1 mL, the left image is $\times 1.00$ k and the inset image is $\times 10.0$ k; (e,f) 2 mL/1 mL/2 mL, the left image is $\times 1.00$ k and the inset image is $\times 10.0$ k) before being treated with the alcoholic vapor with a low molecular weight.

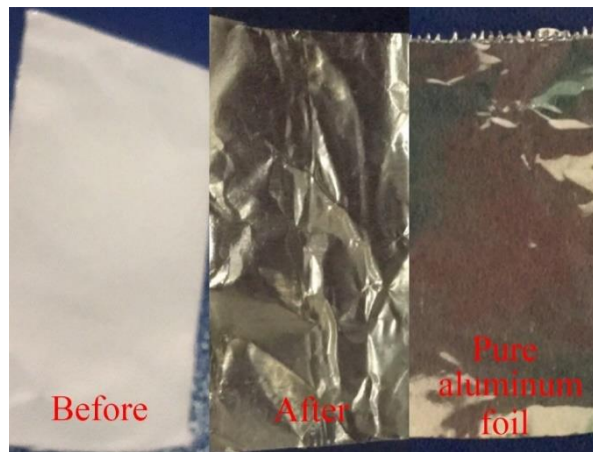


Figure 5. The PLA/shellac/PLA sandwich-structural membrane changes from opaque to transparent after treated with the alcoholic vapor with a low molecular weight. (The PLA/shellac/PLA sandwich-structural membrane was on the pure aluminum foil).

The shellac resin is not a single compound but consists of an intimate mixture of several polar and non-polar components, e.g., five hydroxyl groups including vicinal hydroxyl group, one carboxyl group, in free state, three ester groups, one double bond and one partly masked aldehyde group, and the probable linkages ester, acylal, acetal and ether in an average molecule [15]. The resinous characteristics are believed to be due to the association of components through the hydrogen bonds, which also make shellac react with various monohydric alcohols *viz.*, ethyl alcohol, butyl alcohol, allyl alcohol and dihydric alcohols to form ethers [15]. This is quite different from the PLA in terms of the solubilities in different solvents. The chemical structures of three main components of shellac are shown in Figure 6 [17] and the chemical structure of the main component of poly (lactic acid) is shown in Figure 7 [18].

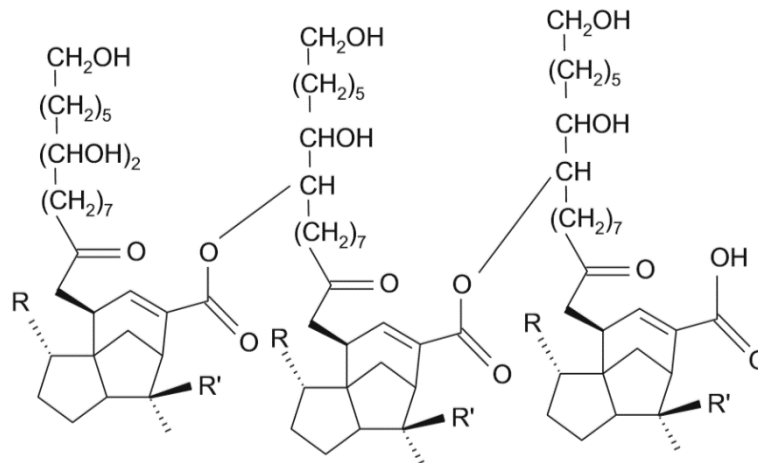


Figure 6. The chemical structures of the main components of shellac.

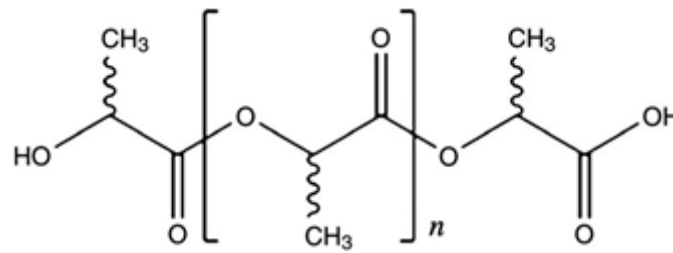


Figure 7. The chemical structure of the main component of poly (lactic acid).

The color change is associated with the mutual solubility of the solute and the solvent, which makes up the mechanism of the sensor for the sandwich structure to react with the alcoholic vapor. The solubility of material in a solvent has been investigated for decades, and the well-recognized theory is based on the energy of mixing ΔE_{mix} , which can be expressed in terms of the following equations [19],

$$\Delta E_{mix} = \phi_1 \phi_2 V_m (\delta_1 - \delta_2)^2 \quad (1)$$

$$\text{C.E.D.} = \frac{\Delta E_{vap}}{V_m} = \delta^2 \quad (2)$$

where ϕ_1, ϕ_2 —volume fractions of the components, V_m —average molar volume, δ_1, δ_2 —solubility of the components, C.E.D.—cohesive energy density, ΔE_{vap} —energy of evaporation.

In general, the solubility δ can be further expressed as the summation of three components, i.e., [19],

$$\delta^2 = \delta_d^2 + \delta_p^2 + \delta_h^2 \quad (3)$$

where δ_d —solubility due to the dispersion force, δ_p —solubility due to the dipole forces, δ_h —solubility due to the hydrogen bonds.

Correspondingly, the three factors can be combined into an enthalpy correction parameter χ_H , i.e., [19],

$$\chi_H = \frac{V_m}{RT} \left[(\delta_{d1} - \delta_{d2})^2 + (\delta_{p1} - \delta_{p2})^2 + (\delta_{h1} - \delta_{h2})^2 \right] \quad (4)$$

here, subscripts 1 and 2 represent the solvent and the polymer, respectively. The smaller the χ_H , the larger the solubility of polymer solute and the solvent.

Now the solubility behaviors of ethanol to PLA and shellac can be illustrated, respectively. The solubility parameter of ethanol to PLA is 78.1 ($\delta_d^2 + \delta_p^2$) since the PLA has no hydrogen bond existed in its chemical structure, while to shellac is 168 ($\delta_d^2 + \delta_p^2 + \delta_h^2$) since there are plenty of hydrogen bonds existed in the chemical structure of shellac [16]. In addition, the molar attraction constants for PLA and shellac are quite different. The molar attraction constant ΣF can be expressed as [20–22],

$$\Sigma F = \delta V_m = V_m (\text{C.E.D.})^2 \quad (5)$$

The ΣF for PLA is 799 cal^{1/2}·c.c.^{1/2}, while for shellac is over 2000 cal^{1/2}·c.c.^{1/2} on average [20–22].

In fact, the PLA is not dissolved in ethanol due to the polarity of PLA, while the ethanol is a weak polar solvent, which is different from DMF, a strong polar solvent. Since the ethanol has good solubility to the shellac, thus the shellac can be used to sense the ethanol quantity in terms of the solubility of ethanol to shellac. The resin properties of shellac are believed to be due to the hydrogen bonding of the components. The resin components of shellac, soft resin, and hard resin all contain hydroxyl acids, and their polar groups are present at the interface of the molecules [15]. Therefore, when the shellac encounters the alcoholic vapor with a low molecular weight, it can form hydrogen bonds with the alcoholic vapor and dissolution occurs. The alcoholic vapor with a low molecular weight contacts with the shellac membrane through the pores of the PLA membrane. The strong interaction of hydrogen bonds between the polar groups makes the PLA/shellac/PLA sandwich-structural membrane very

sensitive to the alcoholic vapor with a low molecular weight. When the composite nanofiber membrane is treated with the alcoholic vapor with a low molecular weight, the shellac nanofiber membrane layer dissolves and slowly passes through the gap between the PLA fiber membranes until a gap-filling coating is formed on the surface of the membrane, which reduces the light scattering of the membrane and increases the transparency of the membrane. The change of transparency can be used to detect the alcoholic vapor.

3.2. Influence of the Vapor Treatment on the Structure and Transparency

The XRD patterns of the PLA nanofibers before and after the alcoholic treatment are almost the same, indicating that the PLA structures do not change during the treatment.

Moreover, the chemical bonds of the membrane can be analyzed by FTIR spectroscopy. Comparing the spectra of the films before and after the alcoholic treatment, it was found that the normalized spectra did not change significantly. In Figure 8, the position of the peak does not change significantly, but the intensities of the peaks change slightly. In order to investigate whether the functional groups of the membrane undergo chemical changes after alcoholic treatment with a low molecular weight, the PLA membranes were examined by ATR-FTIR, which is an approach to test the chemical bonds via molecular vibration and rotation after the infrared light interacting with the molecules. As shown in Figure 8, the peak at 1753 cm^{-1} is a stretching vibration mode of carbon-oxygen double bond (C=O), because the PLA contains the functional group of aliphatic carbonate esters. The peak at $1183\text{--}1088\text{ cm}^{-1}$ is the stretching vibration mode of carbon-oxygen-carbon ester group (C-O-C) [23–26]. The characteristic peak from the carbonyl groups of aliphatic carboxylic acids (C=O stretching vibration) at 1711 cm^{-1} in spectrum of the shellac nanofibers does not change before and after the treatment [27]. The peaks at 2929 cm^{-1} and 1458 cm^{-1} denote the $-\text{CH}_2$ shear vibration absorption and the $-\text{CH}_2$ symmetric bending vibration absorption overlap peak, respectively [28]. This shows that the shellac contains the functional group of aliphatic hydrocarbons. The O-H bending vibration is identified at 1250 cm^{-1} [29]. The absorption bands at $1250\text{--}1039\text{ cm}^{-1}$ may be due to the stretching vibrations of C-O and C-C bonds [30]. For PLA/shellac/PLA membranes, the characteristic peaks from the shellac completely overlap with the absorption bands of PLA, and thus these bands are not available for differentiation.

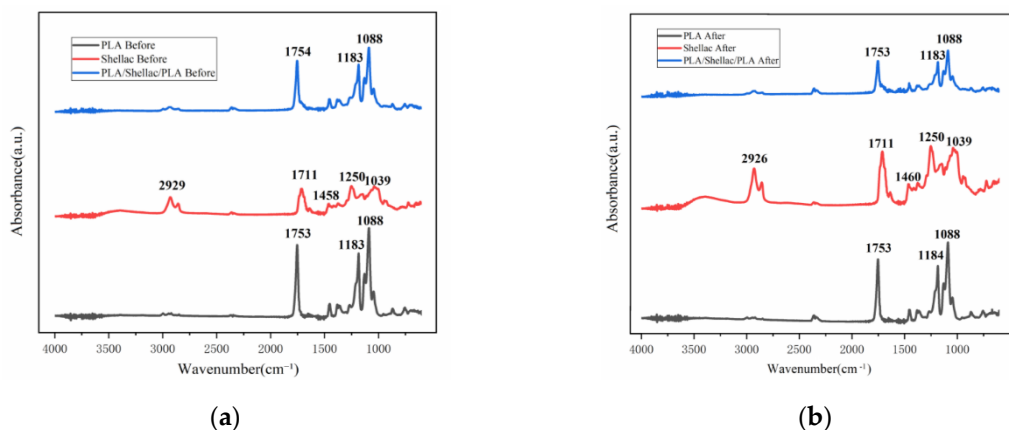


Figure 8. (a) The normalized attenuated total reflection-Fourier transform infrared spectrometer (ATR-FTIR) spectra of samples prepared before treated with the alcoholic vapor with a low molecular weight; (b) the ATR-FTIR spectra of samples prepared after treated with the alcoholic vapor with a low molecular weight.

Figure 9 shows the transparency spectra of PLA/shellac/PLA sandwich structural membrane before and after the treatment with alcohol. One can see that in the whole visible optical range the membrane after the treatment with alcohol has a higher transparency. Also, the wavelength does not affect the transparency significantly.

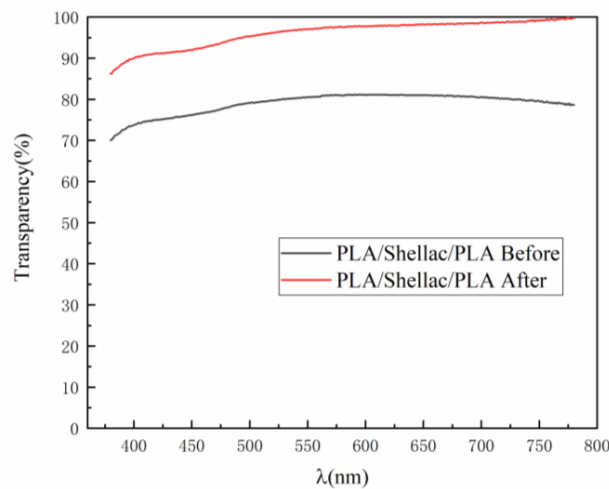


Figure 9. Transparency spectra of PLA/shellac/PLA sandwich structural membrane in the visible optical range.

3.3. Alcoholic Vapor-Sensing Characterization

In this part, we aligned the laser to the surface of the photoresistor and then injected 100 mL of the alcohol reagent into a specific transparent apparatus to form an alcoholic vapor atmosphere at 25 °C. The sample was then placed in this apparatus and the membrane was placed with 5 cm in distance directly above the photoresistor. By measuring the change of the resistance of the photoresistor, the transparency of the PLA/shellac/PLA sandwich-structure membrane in alcoholic vapor with a low molecular weight was discussed. The properties after the alcoholic treatment are listed in Table 1 [31]. As mentioned above, the experiment was carried out in a glove box. The photoresistor was connected to a multimeter, which was connected to the computer to record the data of resistance change in real-time. Figure 10 shows the response of the PLA/shellac/PLA (1 mL/1 mL/1 mL) sandwich-structural membrane to the alcoholic vapor with a low molecular weight, including the methanol and ethanol over time at 25 °C. The *y*-axis is the normalized resistance change:

$$\frac{\Delta R}{R_0} \times 100(\%) = \frac{[R_0 - (R - R_{PR})]}{R_0} \times 100(\%) \quad (6)$$

here *R* stands for the resistance of the photoresistor when the laser passes through the membrane; *R*₀ denotes the resistance of the photoresistor in the absence of laser light; *R*_{PR} is the resistance of the photoresistor when it is directly illuminated by the laser without any absorption.

Table 1. The properties of two alcohols with a low molecular weight.

Solvents	Molar Mass (g/mol)	Molar Volume (cm ³ /mol)	δ _h [*] (MPa) ^{1/2}
Methanol	32.04	40.7	22.3
Ethanol	46.07	58.5	19.4

(*δ² = δ_d² + δ_p² + δ_h², where δ: solubility parameter, δ_d: dispersion term, δ_p: polar term, and δ_h: hydrogen term. δ_h denotes the energy from hydrogen bonds between molecules.)

As shown in Figure 5, when the sandwich structure is exposed to the methanol and the ethanol respectively, the PLA/shellac/PLA sandwich-structural membrane gradually becomes transparent, then the laser light intensity passing through the membrane increases, the resistance of the photoresistor will decrease, thus the resistance change rate will increase accordingly. Finally the resistance change rate will be saturated for a long period of time, e.g., 300 s.

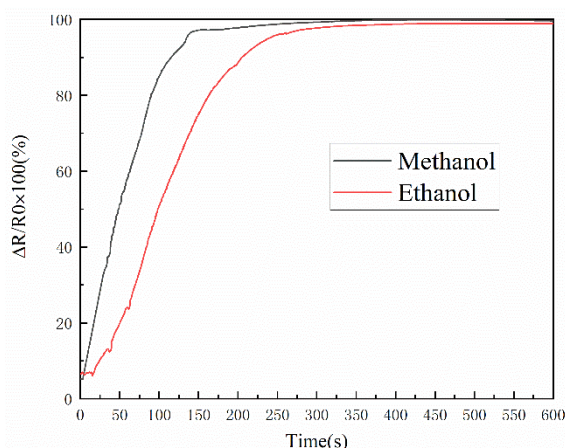


Figure 10. The resistance change rate as a function of time for the PLA/shellac/PLA (1 mL/1 mL/1 mL) sandwich-structural membrane subject to the alcoholic vapor with a low molecular weight.

Compared to the ethanol, the methanol vapor showed faster and larger change rates of resistance. Among the alcoholic vapors, the methanol vapor exhibits a higher value in the normalized resistance change than the ethanol vapor. It is critical for the sandwich structural membrane to distinguish the methanol, ethanol and other alcohols. It was found that the response time is one of the selective methods. Especially, for a 10% of change rate of reduction of the resistance, the response time is 5 s for methanol, and ~25 s for ethanol. The response time depends on the expansion of the shellac in the sandwich structure to the alcohol, e.g., explosion surface area. One can enlarge the expansion area in terms of the porous structure of the PLA on the surface of shellac, the reduction of thickness of the PLA to reduce the contact distance of alcohol to the shellac, as well as enhancement of the capillary force of the porous PLA.

As shown in Table 1 [31], the molar volume of methanol was $40.7 \text{ cm}^3/\text{mol}$, which is much lower than ethanol. In addition, the solubility of the polar part of methanol is larger than the ethanol. That can make the shellac form hydrogen bonds with the methanol much easier and faster than the ethanol. Therefore, the reaction rate of the methanol vapor with the membrane is much faster than the ethanol vapor and the composite membrane has a much smaller response time for the methanol vapor than the ethanol. Thus, the methanol vapor could make the membrane more transparent than the ethanol vapor.

In order to examine the response of different proportions of composite films to the alcoholic vapors with a low molecular weight, the response with different shellac contents in PLA/shellac/PLA sandwich-structural membranes were tested to the ethanol vapor. Figure 11 shows the response of relative resistance change rate to ethanol vapor as a function of time for the PLA/shellac/PLA sandwich-structural membrane with different shellac contents at $25 \text{ }^\circ\text{C}$.

As shown in Figure 11, the content of PLA is set as constant, when the shellac content increases and the ratio of the total content of PLA to the content of shellac is less than 2, the normalized resistance change rate decreases. This indicates that during the treatment of alcoholic vapor with a low molecular weight, when the content of PLA is constant, the increase of shellac content will reduce the transparency of the treated membrane. However, there was no significant change in the response time of the membrane to alcoholic vapor with a low molecular weight. Therefore, changing the shellac content in the PLA/shellac/PLA sandwich-structural membrane does not have a significant impact on the response time of the composite membrane to alcoholic vapor with a low molecular weight.

To further test the response to different concentration of methanol (ethanol) in water solution, we designed a setup in which the alcohol solution was atomized using an atomizing generator and passed through a box to reach the PLA/shellac/PLA sandwich-structural membrane. At the same time, the laser was laterally passing through the sandwich and reaching the photoresistor. The resistance change was recorded using a multimeter and computer. The results are shown in Figure 12. From the figure, one can see that the smallest concentration of methanol (ethanol) in water is 10 wt% (10 wt%),

which lead to a normalized resistance change of 67.09% (64.57%) for methanol (ethanol), compared to the value of 99.62% (98.91%) for 100 wt% (100 wt%) of methanol (ethanol).

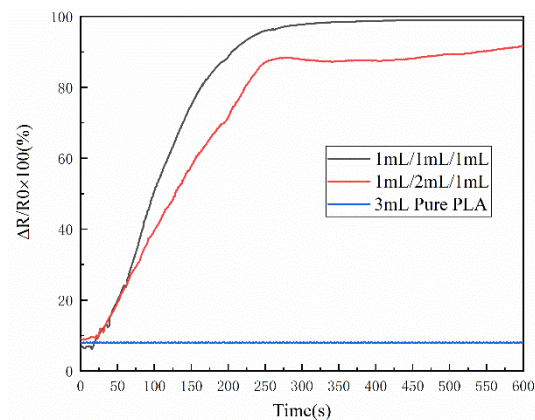


Figure 11. The response to ethanol vapor for the PLA/shellac/PLA sandwich-structural membrane with different shellac contents.

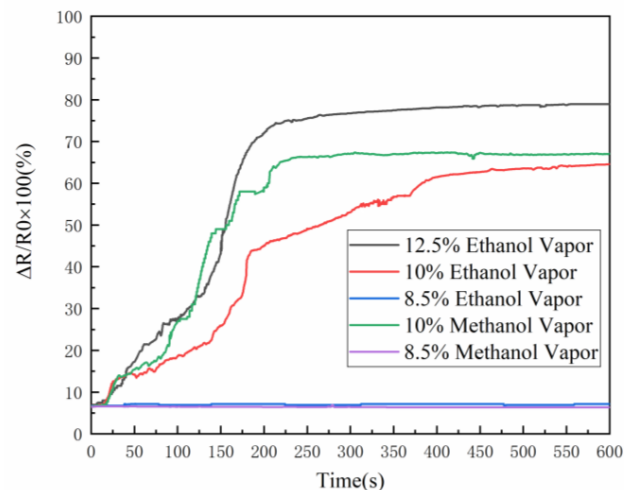


Figure 12. Relative photoresistance change as a function of time for different concentrations of methanol (ethanol) in d.i. water.

4. Conclusions

In conclusion, a PLA/shellac/PLA sandwich composite electrospun fiber membrane was prepared for sensing alcoholic vapor with a low molecular weight. In addition, the morphology, structure, chemical properties and response of a PLA/shellac/PLA sandwich composite membrane to the alcoholic vapor with a low molecular weight were examined. It was found that the PLA/shellac/PLA sandwich composite membrane exhibited a good response to the alcoholic vapor with a low molecular weight, especially for the methanol vapor. The transparency of the PLA/shellac/PLA sandwich membrane increases upon exposure to the alcoholic vapor with a low molecular weight. The morphology of the PLA nanofiber membrane on the PLA/shellac/PLA sandwich composite membrane does not change, however, the shellac nanofiber membrane dissolved and slowly passed through the gap between the PLA fiber membranes. Until a gap-filling coating was formed on the surface of the film, the light scattering of the film was reduced, and the transparency of the film was enhanced. Therefore, the PLA/shellac/PLA sandwich composite membrane shows great potential for alcoholic vapor sensing.

Author Contributions: Conceptualization, S.-G.L. and S.-C.W.; methodology, S.-C.W.; formal analysis, S.-G.L. and S.-C.W.; investigation, S.-C.W., J.-W.L., Y.-B.Y., T.T. and B.L.; data curation, S.-C.W.; writing—original draft preparation, S.-C.W. and J.-W.L.; writing—review and editing, S.-G.L.; funding acquisition, S.G.L.

Funding: This work was supported by the Natural Science Foundation of China [Grant No. 51372042, 51872053], the Guangdong Provincial Natural Science Foundation [2015A030308004], and the NSFC-Guangdong Joint Fund [Grant No. U1501246].

Conflicts of Interest: The authors declare no conflict of interest.

References

1. Linnerud, I.; Kaspersen, P.; Jaeger, T. Gas monitoring in the process industry using diode laser spectroscopy. *Appl. Phys. B-Lasers Opt.* **1998**, *67*, 297–305. [[CrossRef](#)]
2. Vaseashta, A.; Vaclavikova, M.; Vaseashta, S.; Gallios, G.; Roy, P.; Pummakarnchana, O. Nanostructures in environmental pollution detection, monitoring, and remediation. *Sci. Technol. Adv. Mater.* **2007**, *8*, 47–59. [[CrossRef](#)]
3. Di Natale, C.; Paolesse, R.; Martinelli, E.; Capuano, R. Solid-state gas sensors for breath analysis: A review. *Anal. Chim. Acta* **2014**, *824*, 1–17. [[CrossRef](#)] [[PubMed](#)]
4. Machado, R.F.; Laskowski, D.; Deffenderfer, O.; Burch, T.; Zheng, S.; Mazzone, P.J.; Mekhail, T.; Jennings, C.; Stoller, J.K.; Pyle, J.; et al. Detection of lung cancer by sensor array analyses of exhaled breath. *Am. J. Respir. Crit. Care Med.* **2005**, *171*, 1286–1291. [[CrossRef](#)] [[PubMed](#)]
5. Bevenot, X.; Trouillet, A.; Veillas, C.; Gagnaire, H.; Clement, M. Hydrogen leak detection using an optical fibre sensor for aerospace applications. *Sens. Actuator B-Chem.* **2000**, *67*, 57–67. [[CrossRef](#)]
6. Mirzaei, A.; Janghorban, K.; Hashemi, B.; Bonyani, M.; Leonardi, S.G.; Neri, G. Highly stable and selective ethanol sensor based on α -Fe₂O₃ nanoparticles prepared by Pechini sol-gel method. *Ceram. Int.* **2016**, *42*, 6136–6144. [[CrossRef](#)]
7. Yebo, N.A.; Lommens, P.; Hens, Z.; Baets, R. An integrated optic ethanol vapor sensor based on a silicon-on-insulator microring resonator coated with a porous ZnO film. *Opt. Express* **2010**, *18*, 11859–11866. [[CrossRef](#)]
8. Hu, P.G.; Du, G.J.; Zhou, W.J.; Cui, J.J.; Lin, J.J.; Liu, H.; Liu, D.; Wang, J.Y.; Chen, S.W. Enhancement of Ethanol Vapor Sensing of TiO₂ Nanobelts by Surface Engineering. *ACS Appl. Mater. Interfaces* **2010**, *2*, 3263–3269. [[CrossRef](#)]
9. Patel, N.G.; Patel, P.D.; Vaishnav, V.S. Indium tin oxide (ITO) thin film gas sensor for detection of methanol at room temperature. *Sens. Actuator B-Chem.* **2003**, *96*, 180–189. [[CrossRef](#)]
10. Subbiah, T.; Bhat, G.S.; Tock, R.W.; Parameswaran, S.; Ramkumar, S.S. Electrospinning of nanofibers. *J. Appl. Polym. Sci.* **2005**, *96*, 557–569. [[CrossRef](#)]
11. Reneker, D.H.; Chun, I. Nanometre diameter fibres of polymer, produced by electrospinning. *Nanotechnology* **1996**, *7*, 216–223. [[CrossRef](#)]
12. Bazrafshan, Z.; Stylios, G.K. One-Step Fabrication of Three-Dimensional Fibrous Collagen-Based Macrostructure with High Water Uptake Capability by Coaxial Electrospinning. *Nanomaterials* **2018**, *8*, 803. [[CrossRef](#)] [[PubMed](#)]
13. Garlotta, D. A literature review of poly(lactic acid). *J. Polym. Environ.* **2001**, *9*, 63–84. [[CrossRef](#)]
14. Popelka, S.; Machova, L.; Rypacek, F. Adsorption of poly(ethylene oxide)-block-poly lactide copolymers on polylactide as studied by ATR-FTIR spectroscopy. *J. Colloid Interface Sci.* **2007**, *308*, 291–299. [[CrossRef](#)]
15. Sharma, S.K.; Shukla, S.K.; Vaid, D.N. Shellac-Structure, Characteristics & Modification. *Def. Sci. J.* **2014**, *33*, 261–271.
16. Sawalha, H.; Schroen, K.; Boom, R. Biodegradable polymeric microcapsules: Preparation and properties. *Chem. Eng. J.* **2011**, *169*, 1–10. [[CrossRef](#)]
17. Ma, K.; Qiu, Y.P.; Fu, Y.Q.; Ni, Q.Q. Electrospun sandwich configuration nanofibers as transparent membranes for skin care drug delivery systems. *J. Mater. Sci.* **2018**, *53*, 10617–10626. [[CrossRef](#)]
18. Ana, P.S.I.; Manuel, L.A.; N ria, C.; Rafael, L.B.; Jos , A.T. Drug delivery systems using sandwich configurations of electrospun poly(lactic acid) nanofiber membranes and ibuprofen. *Mater. Sci. Eng. C-Mater. Biol. Appl.* **2013**, *33*, 4002–4008.
19. Koenhen, D.M.; Smolders, C.A. The determination of solubility parameters of solvents and polymers by means of correlations with other physical quantities. *J. Appl. Polym. Sci.* **1975**, *19*, 1163–1179. [[CrossRef](#)]
20. Small, P.A. Some factors affecting the solubility of polymers. *J. Appl. Chem.* **1953**, *3*, 71–80. [[CrossRef](#)]
21. Hoy, K. New values of the solubility parameters from vapor pressure data. *J. Paint Technol.* **1970**, *42*, 76–118.

22. Burrell, H. Solubility parameters for film formers. *Off. Dig.* **1955**, *369*, 726–758.
23. Liang, J.W.; Gajula, P.; Wang, S.C.; Wu, J.L.; Lu, S.G. Enhancement of the Oil Absorption Capacity of Poly(Lactic Acid) Nano Porous Fibrous Membranes Derived via a Facile Electrospinning Method. *Appl. Sci.* **2019**, *9*, 1014. [[CrossRef](#)]
24. Agarwal, M.; Koelling, K.W.; Chalmers, J.J. Characterization of the Degradation of Polylactic Acid Polymer in a solid substrate environment. *Biotechnol. Prog.* **1998**, *14*, 517–526. [[CrossRef](#)]
25. Yang, S.-L.; Wu, Z.-H.; Yang, W.; Yang, M.-B. Thermal and mechanical properties of chemical crosslinked polylactide (PLA). *Polym. Test.* **2008**, *27*, 957–963. [[CrossRef](#)]
26. Thanki, P.N.; Dellacherie, E.; Six, J.-L. Surface characteristics of PLA and PLGA films. *Appl. Surf. Sci.* **2006**, *253*, 2758–2764.
27. Ahn, J.Y.; Chung, W.J.; Pinnau, I.; Guiver, M.D. Poly sulfone/silica nanoparticle mixed-matrix membranes for gas separation. *J. Membr. Sci.* **2008**, *314*, 123–133. [[CrossRef](#)]
28. Zumbühl, S.; Hochuli, A.; Soulier, B.; Scherrer, N.C. Fluorination technique to identify the type of resin in aged vanishes and lacquers using infrared spectroscopy. *Microchem. J.* **2017**, *134*, 317–326. [[CrossRef](#)]
29. Brajnicov, S.; Bercea, A.; Marascu, V.; Matei, A.; Mitu, B. Shellac Thin Films Obtained by Matrix-Assisted Pulsed Laser Evaporation (MAPLE). *Coatings* **2018**, *8*, 275. [[CrossRef](#)]
30. Licchelli, M.; Malagodi, M.; Somaini, M.; Weththimuni, M.; Zanchi, C. Surface treatments of wood by chemically modified shellac. *Surf. Eng.* **2013**, *29*, 121–127. [[CrossRef](#)]
31. Choi, J.; Park, E.J.; Park, D.W.; Shim, S.E. MWCNT-OH adsorbed electrospun nylon 6,6 nanofibers chemiresistor and their application in low molecular weight alcohol vapours sensing. *Synth. Met.* **2010**, *160*, 2664–2669. [[CrossRef](#)]



© 2019 by the authors. Licensee MDPI, Basel, Switzerland. This article is an open access article distributed under the terms and conditions of the Creative Commons Attribution (CC BY) license (<http://creativecommons.org/licenses/by/4.0/>).